

Paramagnetic effect in $\text{YBa}_2\text{Cu}_3\text{O}_{7-x}$ grain-boundary junctions

E. Il'ichev,^{1,*} F. Tafuri,^{2,3} M. Grajcar,^{4,†} R. P. J. IJsselsteijn,¹ J. Weber,¹ F. Lombardi,⁵ and J. R. Kirtley³

¹*Institute for Physical High Technology, P.O. Box 100239, D-07702 Jena, Germany*

²*INFN-Cohrentia Dip. Ingegneria, Seconda Università di Napoli, 81031 Aversa (CE), Italy*

³*IBM Watson Research Center, Route 134 Yorktown Heights, New York 10598, USA*

⁴*Friedrich Schiller University, Institute of Solid State Physics, D-07743 Jena, Germany*

⁵*MINA-Chalmers University of Technology and Goteborg University, S-41296 Goteborg, Sweden*

(Received 17 January 2003; published 29 July 2003)

A detailed investigation of the magnetic response of $\text{YBa}_2\text{Cu}_3\text{O}_x$ grain-boundary Josephson junctions has been carried out using both radio-frequency measurements and scanning superconducting quantum interference device microscopy. In a nominally zero-field-cooled regime we observed a paramagnetic response at low external fields for 45° asymmetric grain boundaries. We argue that the observed phenomenology results from the d -wave order-parameter symmetry and depends on Andreev bound states.

DOI: 10.1103/PhysRevB.68.014510

PACS number(s): 74.50.+r, 74.40.+k, 73.23.Hk, 85.25.Cp

Superconductors below the transition temperature T_c usually expel an external magnetic field. This phenomenon, known as the Meissner effect, leads to diamagnetism. It was therefore quite unexpected that a paramagnetic Meissner effect (PME) was observed in a field-cooled regime for ceramic $\text{Bi}_2\text{Sr}_2\text{CaCu}_2\text{O}_8$ (Refs. 1 and 2) (BiSCCO). For an explanation, it was proposed that below T_c there are randomly distributed spontaneous orbital currents in the sample.^{1,3} These currents can be oriented by an external magnetic field, providing a paramagnetic signal. Sigrist and Rice⁴ pointed out that the spontaneous orbital currents can be caused by a $d_{x^2-y^2}$ -wave symmetry of the superconducting state. Indeed, the d -wave scenario predicts the existence of Josephson junctions (JJs) in which the Josephson energy reaches a minimum for a phase difference across the junction at $\phi = \pi$ (π contact). In ceramic high- T_c superconductors (HTSs) the grains can form loops which contain odd numbers of π contacts, so-called frustrated loops.⁴ In such a system the energy is minimized by a configuration with a spontaneous current flowing in the loop.⁵ In particular, for a π contact with a “conventional” current-phase relationship $I = I_c \sin(\phi + \pi)$ inserted in a loop, the gain in Josephson energy exceeds the loss of magnetic energy when the parameter β satisfies $\beta = 2\pi L I_c / \Phi_0 > 1$, where Φ_0 is the flux quantum, I_c is the critical current, and L is a loop inductance. However, a paramagnetic signal in the field-cooled regime has also been observed for conventional superconductors.^{6,7}

In order to distinguish between different origins of paramagnetism Rice and Sigrist⁸ proposed to detect spontaneous orbital currents with the use of a superconducting quantum interference device (SQUID) microscope for zero-field-cooled samples. In a granular BiSCCO sample exhibiting a paramagnetic signal, spontaneous magnetization has indeed been observed.⁹ The PME and the presence of spontaneous currents therefore represent two of the main features induced by the d -wave order-parameter symmetry in HTSs. A comparative study of these phenomena on a more controlled system, such as a grain-boundary (GB) line, could shed additional light on the relation between these effects and their influence on the properties of the grain-boundary Josephson junctions (GBJJs).

In this paper, we give evidence of paramagnetic behavior for zero-field-cooled asymmetric 45° $\text{YBa}_2\text{Cu}_3\text{O}_x$ (YBCO) GBJJs. The paramagnetic signal, that has been previously observed in two-dimensional systems, has been in this case detected in a single GB line and related to basic mechanisms in HTS JJs. Apart from conventional transport properties and scanning SQUID microscopy (SSM) measurements, we exploited radio-frequency measurements, which are very sensitive and provide a direct test for paramagnetic signals as demonstrated below. This is a further manifestation of the d -wave nature of the order parameter, but it is also relevant for the understanding of transport across GBJJs and in particular on the incidence of Andreev bound states.

The idea of the rf measurements is the following. The sample of interest is inductively coupled to a high-quality (quality factor $Q \approx 300$) parallel resonant circuit of inductance L_T and capacitance C_T . Experimentally this is realized by a “flip chip” configuration—the sample is placed on the top of a small solenoid coil perpendicular to its axis. For such an arrangement, the effective impedance of the tank circuit coupled to the sample is a function of the external magnetic field H_e applied to the sample. This field consists of a dc and an rf component as induced by a current I_{dc} (in fact of very low frequency) and an rf oscillating current I_{rf} in the tank coil, hence $H_e = H_{dc} + H_{rf}$. In order to avoid the nucleation of rf “vortices” and other nonlinear effects, the amplitude of H_{rf} is small, so that $H_{rf} \ll H_{c1}$, H_{dc} where H_{c1} is the first critical field, therefore $H_e \cong H_{dc}$. If $L_{eff}(H_{dc})$ and $R_{eff}(H_{dc})$ are the effective inductance and the effective resistance of the tank circuit-sample system, respectively, the phase angle α between the drive current I_{rf} and the tank voltage U is given by

$$\tan \alpha = \frac{1}{R_{eff}(H_{dc})} \cdot \left[\frac{1}{\omega C_T} - \omega L_{eff}(H_{dc}) \right]. \quad (1)$$

It follows from Eq. (1) for $H_{dc} = 0$ and at the resonance frequency $\omega_0 = 1/\sqrt{L_{eff}(0)C_T}$ that the parameter α is zero. Therefore, by monitoring α as a function of H_{dc} at the frequency ω_0 , the $L_{eff}(H_{dc})$ dependence can be obtained [note that $R_{eff}(H_{dc})$ dependence is controlled independently, by

measuring the quality factor Q of the tank circuit-sample system]. If $R_{eff} = R_T$ does not depend on H_{dc} then $\tan \alpha$ can be written as

$$\tan \alpha = -k^2 Q \chi_m, \quad (2)$$

where k is the coupling coefficient between the tank coil and the sample, and χ_m is the ac magnetic susceptibility of the sample. In the experiments, we are obviously interested in the regime $\chi_m \neq \text{const}$, the only configuration able to provide significant information. Let us analyze Eq. (2) near $H_e = 0$. When the supercurrent induced by an externally applied field is diamagnetic, a change of $\chi_m < 0$ will result in a local maximum in $\alpha(H_e)$. Similarly, a local minimum of the $\alpha(H_e)$ curve indicates a paramagnetic response ($\chi_m > 0$).

The simplest system which exhibits a similar behavior is the well-known rf SQUID. The sensor of this device is a Josephson junction inserted in a superconducting loop. If the inductance L of the loop is relatively small (so that $\beta < 1$), the $\alpha(H_{dc})$ dependence has a local maximum at $H_{dc} = 0$ (see, for example, Ref. 11). Due to the induced current in the sensor, the magnetic flux Φ_i inside the loop satisfies $\Phi_i < \Phi_e$, where Φ_e is an applied external flux. Therefore, the magnetic response is diamagnetic. If, instead of a conventional junction, a π contact is inserted in the same sensor, the $\alpha(H_{dc})$ dependence has a local minimum at $H_{dc} = 0$ and $\Phi_i > \Phi_e$, providing a paramagnetic response. The phase shift α can be obtained from Eq. (2) defining $\chi_m = d\Phi_i/d\Phi_e - 1$.¹⁰ The value of $k^2 Q$ allows the estimation of the resolution of the rf measurement, in this case of the order of a few percent of the flux quantum.

As we discussed above, within the framework of the d -wave scenario, extrinsic effects such as faceting can play a relevant role in the determination of the properties of the junctions and can contribute in particular to causing spontaneous currents and/or a paramagnetic effect. In the case of a strongly meandering interface, the GB exhibits a random parallel array of 0 and π contacts. This is somehow the analog of the explanation of the PME in BiSCCO crystals in the one-dimensional case of a GB line (π -loops model). An alternative mechanism of the PME can be given in terms of the midgap states (MGS) and surface properties of d -wave superconductors (MGS model). In this case, the MGS model is valid even for flat interfaces of a d -wave superconductor.

The interplay between the PME and superconductivity, apart from being an interesting topic itself on d -wave-induced effects, may be crucial to improve understanding of transport properties of GBs. It has been demonstrated that GB transport properties strongly depend on the quality of the substrate,¹² the thin film, and the type of growth. This led to apparently conflicting behaviors in a wide spectrum of transport regimes. Zigzag Nb-Au-YBCO junctions isolated the effect of facets by investigating the presence of spontaneous currents and anomalous magnetic patterns.¹³ We intend to reach the other limit by investigating a morphology with nominal, very reduced faceting, and low barrier transparency. To this aim we employed biepitaxial junctions, where ‘‘clean’’ basal plane GBs can be reproducibly obtained.

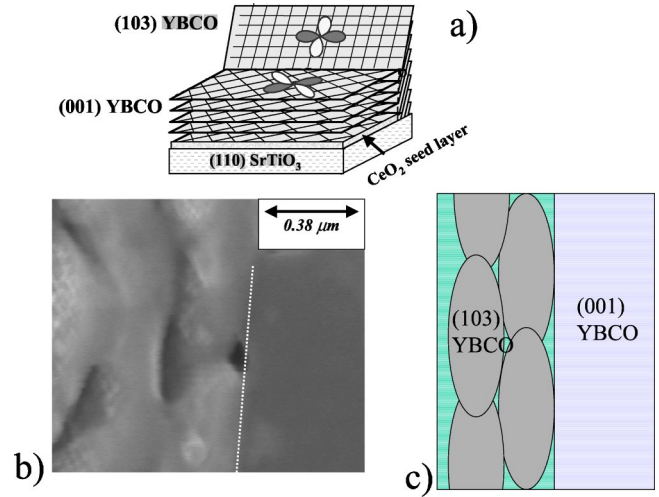


FIG. 1. (Color online) (a) Sketch of the investigated biepitaxial grain boundary where a 45° c -axis tilt accompanies the 45° a -axis tilt; (b) scanning electron microscope image relative to this GB. The elongated grains on the left typical of the (103) growth may generate clean interfaces with reduced faceting, as evident also in (c).

The biepitaxial technique allows the fabrication of various GBJs by growing different seed layers and using substrates with different orientations.^{14,15} In this experiment we have used CeO_2 as a seed layer material deposited on (110) SrTiO_3 substrates. Details of the fabrication procedure can be found elsewhere.¹⁵ YBCO grows along the [001] direction on CeO_2 seed layers, while it grows along the [103]/[013] direction on SrTiO_3 substrates. By using CeO_2 as a seed layer we were able to induce a 45° rotation of the a - b plane of the YBCO with respect to the in-plane direction of the SrTiO_3 substrate, and as a consequence the π contact is formed.¹⁶ The measurements shown below are for the case in which a 45° c -axis tilt accompanies the 45° a -axis tilt [Fig. 1(a)]. This configuration, in principle, leads to interfaces where effects due to faceting can be very reduced, as shown, for instance, in the scanning electron microscope image of Fig. 1(b), and the relative sketch of Fig. 1(c). For biepitaxial junctions in the tilt case,¹⁴ the YBCO growth kinetics and the junction interface orientation determine that the long side of the [103] grains faces the c -axis counterelectrode, and this leads to a more controlled GB (basal plane GB). This has been confirmed by cross-section transmission electron microscope investigations.¹⁴

The sample originally had a typical SQUID geometry with a central hole of $50 \mu\text{m} \times 50 \mu\text{m}$. rf and SSM measurements were performed on a configuration where one of junctions was removed and the other was reduced to about $60 \mu\text{m}$.

Results of rf measurements as a function of an externally applied magnetic field at the temperature range from $T = 4.2$ K up to 40 K are presented in Fig. 2 for nominally zero-field-cooled samples (the rest field is below 0.2 mOe). The sharp minimum at $H_{dc} = 0$ in Fig. 2 represents an unusual feature with respect to most GB systems, which exhibit a maximum for zero field. The minima at a finite magnetic

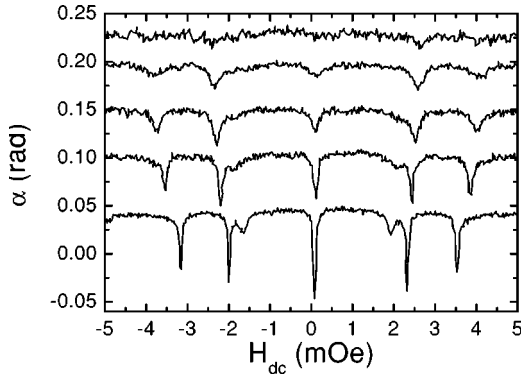


FIG. 2. The phase angle α as a function of the external magnetic field applied perpendicular to the substrate of a $65\text{-}\mu\text{m}$ -wide bridge across an asymmetric 45° $\text{YBa}_2\text{Cu}_3\text{O}_x$ grain boundary. From top to bottom the data correspond to $T=40, 30, 20, 10,$ and 4.2 K. The data are vertically shifted for clarity.

field are originated by the redistribution of the magnetic flux into the GB, as extensively discussed in Ref. 17.

According to the discussion above, the minimum of α at $H_{dc}=0$ is direct evidence of paramagnetic behavior of this type of GB. Furthermore the paramagnetic response was absent after the removal of YBCO from the GB region, demonstrating that the effect is only due to the GB. In other words we just repeated the same measurement on the same sample after removing only a narrow region of YBCO along the grain-boundary line in order to prove that the paramagnetic signal was caused by the grain boundary and not by any uncontrolled environmental reason (substrate or sample holder) or possible impurities in the YBCO thin film far from the GB line. The absence of hysteresis for $\alpha(H_{dc})$ dependence with respect to external field means that there is no spontaneous surface current or flux generated in the GB. This is analogous to the situation in a rf SQUID with π contact for $\beta < 1$. In the case of finite fluctuations the jumps of Φ_i can occur with a certain probability when Φ_e falls in a hysteresis region.¹⁸ When the distribution width of the jump probability is larger than the width of the hysteresis, the flux jumps many times during the measurements. As a result the apparent time-averaged $\Phi_i(\Phi_e)$ dependence presents a finite slope rather than hysteresis even for $\beta > 1$ (see Fig. 3). This situation has already been observed experimentally.¹⁹

Detailed insight into the problem of the paramagnetic effect and of spontaneous currents in faceted GBs has been provided in Refs. 20 and 21. In this model the current density $j_S(x)$ (x is the coordinate in the plane of the contact) is a random and alternating function of x , $j_c(x) = \langle j_c \rangle [1 + g_0 f(x)]$ with $\langle f(x) \rangle = 0$, $\max[f(x)] = 1$, and $g_0 = \max[j_c(x)/\langle j_c \rangle]$. The length scale l of $g(x)$ variations is of the order of the grain-boundary meandering typically l is in the range of $0.01\text{--}0.1\ \mu\text{m}$.²¹ For a conventional current-phase relationship $j_c(x) = \langle j_c \rangle \sin \varphi(x)$, the properties of the GBJJ are determined by the parameter²⁰ $\gamma = g_0^2 l^2 / 8\pi^2 \Lambda_j^2$. Here $\Lambda_j = (c\Phi_0 / 16\pi^2 \lambda \langle j_c \rangle)^{1/2}$ is the effective Josephson penetration depth and λ is the London penetration depth. Within this model, for $\gamma < 1$ there is no created flux in the GBJJ and the microjunctions stay in a “excited currentless

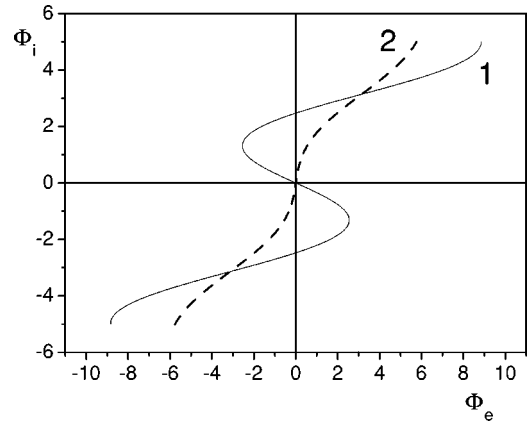


FIG. 3. Schematic drawings of time-averaged magnetic flux inside the GB vs applied magnetic flux (1) without thermal fluctuation and (2) with large thermal fluctuation.

state.”²² In principle, such junctions can exhibit a paramagnetic response. When $\gamma > 1$ there is flux generated in the GBJJ. Qualitatively, this requirement is similar to the condition $\beta > 1$ for the rf SQUID, as discussed above. Thus the same arguments concerning thermal fluctuations can be made for our experiments. If at $\Phi_e = 0$ and $T = 0$ there is spontaneous flux in the GB, one should observe hysteresis of the $\Phi_i(\Phi_e)$ dependence (see Fig. 3, curve 1). However, at finite temperature, fluctuations wash out the hysteresis, therefore there is no spontaneous current (see Fig. 3, curve 2). The above scenario relies on a macroscopic approach to the GB, which is a random array of parallel 0 and π junctions, i.e., the “extrinsic” effect of faceting.

The other possible scenario is based on microscopic arguments, and mainly on mechanisms based on Andreev reflection at the surface.^{23–26} The d -wave symmetry of the gap leads to the formation of the surface state at zero energy (so-called midgap states²⁷). These MGS are degenerate with respect to the direction along the surface of the superconductor ($\pm k_y$). Any mechanism which is able to split the MGS will lower the energy of the system.²⁸ The splitting of the MGS leads to spontaneous currents along the surface and therefore to time-reversal symmetry breaking.

Different mechanisms of the MGS splitting were proposed in the literature (see Ref. 26, and References therein). Apart from suggestions based on the presence of an imaginary component of the order parameter (such as $d \pm is$, see, for example, Ref. 29), there are at least two scenarios based only on pure d -wave symmetry of the order parameter.

The former scenario takes into account the Josephson effect. For an asymmetric 45° GBJJ the energy of the MGS can be written as²³

$$\varepsilon_{\text{MGS}}(\varphi, k_y) = -\text{sgn}(k_y) E_0(\vartheta) \sin(\varphi), \quad (3)$$

where $E_0 = \Delta_L |\Delta_R| D(\vartheta) / \{2|\Delta_L| + D(\vartheta)[|\Delta_R| - |\Delta_L|]\}$, $D(\vartheta)$ is the angle-dependent barrier transparency, and Δ_L , Δ_R are superconducting energy gaps for the angle $\vartheta = \arcsin k_y / k_F$ in the left and right superconductor, respectively. For an asymmetric 45° GBJJ the Josephson energy

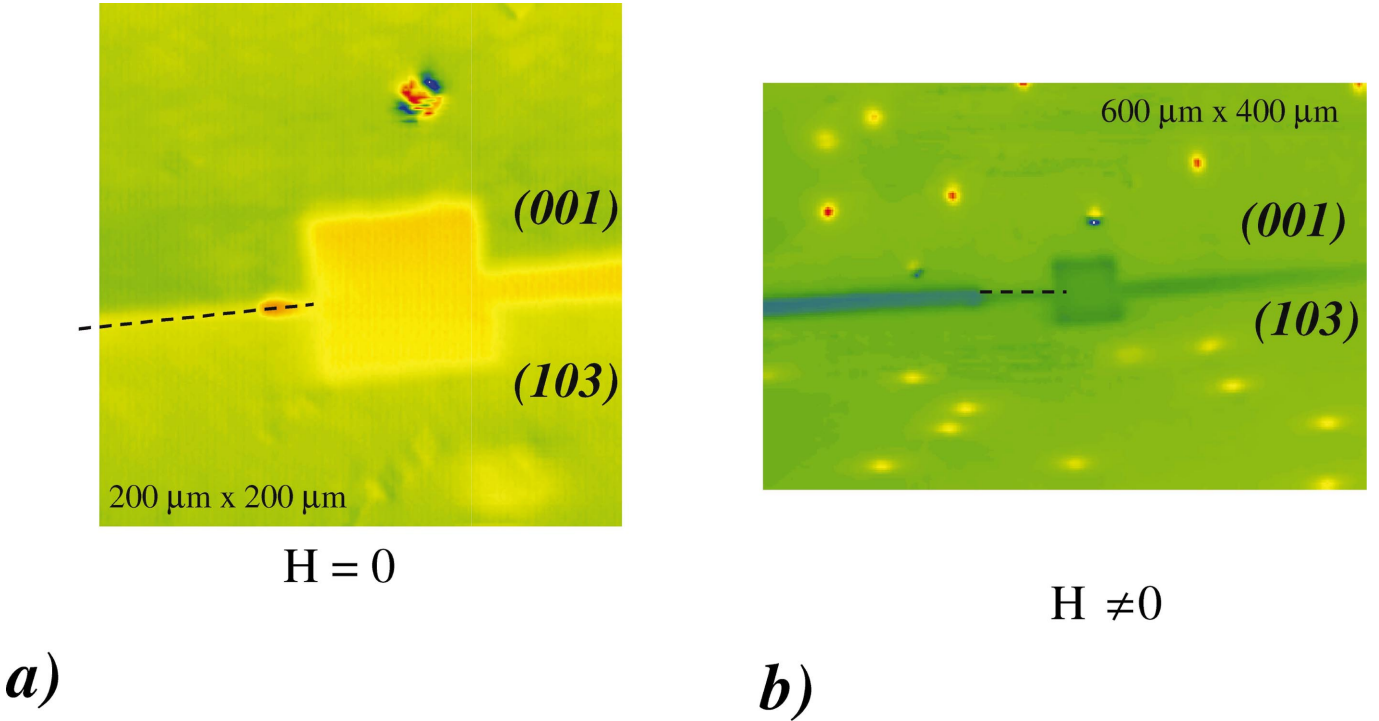


FIG. 4. (Color) Scanning SQUID microscopy image of (a) a $200 \times 200\text{-}\mu\text{m}^2$ area, enclosing the tilt GB; the sample was cooled in zero magnetic field; (b) a $600 \times 400\text{-}\mu\text{m}^2$ area, enclosing the tilt GB; the sample was cooled in a small magnetic field. Both images refer to the sample measured by rf techniques, and the grain-boundary junction is indicated by a dotted line. In all images, taken at $T=4.2$ K, there is no evidence of spontaneous currents. In (b) the superconducting nature of both electrodes is proven by the presence of Abrikosov vortices, which appear elongated in the (103) electrode.

minimum corresponds to the equilibrium phase difference across the junction $\varphi = \pi/2$ which leads to the splitting of the MGS.³⁰ Hence, the spontaneous paramagnetic current flows in the surface layer $\sim \xi_0$. This current is screened by the Meissner supercurrent on the scale of λ and the system pays for the gain in the Josephson energy at the expense of the energy of the magnetic field.

Within the framework of the latter scenario the free surface of a d -wave superconductor has been found to be responsible for the appearance of the paramagnetic effect. In this case the paramagnetic quasiparticle current tries to compensate the Meissner supercurrent.²⁵ As a matter of fact the supercurrent causes a redistribution of quasiparticles in \mathbf{k} space due to the shift $E_{\mathbf{k}} = E_{\mathbf{k}}^0 + \mathbf{p}_{\mathbf{k}} \cdot \mathbf{v}_s$ in the quasiparticle excitation energy, where $E_{\mathbf{k}}^0$ is the excitation energy in the absence of a supercurrent, \mathbf{v}_s is the velocity of the supercurrent, and $\mathbf{p}_{\mathbf{k}}$ is momentum of the quasiparticle. This is obviously relevant for a (110)-oriented HTS surface due to the existence of the MGS.

The key feature for both of the described approaches is the presence of a mechanism able to split the MGS and produce a gap E_0 , or in other words to populate the $\pm k_y$ MGS unequally. This phenomenon is accompanied by a phase transition to a time-reversal symmetry-breaking (TRSB) state. The transition temperature T_{TRSB} can be evaluated and in both approaches T_{TRSB} has been estimated to be below 1 K, in agreement with tunneling experiments.³¹ T_{TRSB} will apparently be the relevant parameter also for the PME. However, in analogy with rf SQUID properties, above T_{TRSB} one

should observe no hysteresis but rather a steep slope of $\Phi_i(\Phi_e)$ at $\Phi_e=0$ (again see Fig. 3). This explains why we observed a PME in a wide temperature range well above the T_{TRSB} values, but no hysteretic behavior.

Additional information has been provided by SSM investigations, which revealed the absence of spontaneous currents, as shown in the SSM images of the GBJJ region in Fig. 4. Figures 4(a) and 4(b) are SSM images of a wide area around the GB in zero-field cooling, and in nonzero-field cooling, respectively, both at $T=4.2$ K. Figure 4(a) confirms in zero-field cooling the absence of any spontaneous magnetization for this sample. This result is different from other measurements of 45° asymmetric bicrystal³² and biepitaxial GBJJs.³³ We attribute this difference to the concomitance of reduced faceting along the GB and the low barrier transparency of this junction, characterized by low values of the critical current density j_C about 10^2 A/cm².³⁴ Figure 4(b) provides evidence of vortices in both the electrodes, and, in particular, of anisotropic vortices in the (103) electrode. As a consequence, it seems not to be the case that the PME is originated by π loops across the GB (π -loops model, see above). Moreover, the observed narrow dip on α vs H_{dc} characteristics at $H_{dc}=0$ (see Fig. 2) requires $\gamma \approx 1$. Simple estimations show that $\gamma \approx 1$ corresponds to critical current densities across the GBJJ of the order of 10^5 A/cm², which seems to be unrealistic, given that the average critical current density for our junction is of the order of 10^2 A/cm². On the other hand the MGS model is apparently consistent with our results.

In conclusion, we have measured the magnetic-field response of an asymmetric 45° grain boundary in a $\text{YBa}_2\text{Cu}_3\text{O}_x$ thin film. The results of these investigations allow us to identify Andreev bound states as the cause of the paramagnetic effect, confirming theoretical predictions. Andreev bound states have been studied in detail theoretically in HTS Josephson junctions and systems. However, due to their extreme localization and stringent survival conditions, experimental detection has been basically confirmed only by one type of measurement, zero-bias anomalies in tunneling spectra.³¹ Our method is complementary and direct, and relies on the comparison of various types of measurements realized on the same samples. The contribution to the exist-

ing state of knowledge on d -wave order-parameter symmetry in HTS's is to demonstrate experimentally the occurrence of bound states through an innovative approach, shedding light on the paramagnetic effect in a different topological configuration.

The authors would like to thank V. Zakosarenko, A. Golubov, and Yu. Barash for numerous illuminating discussions. E.I. and M.G. were partially supported by D-wave Systems Inc. M.G. wants to acknowledge the support of Grant Nos. VEGA 1/9177/02 and APVT-51-021602. This work has been partially supported by the ESF projects "II-Shift" and QUACS.

*Electronic address: ilichev@ipht-jena.de

[†]On leave from Department of Solid State Physics, Comenius University, SK-84248 Bratislava, Slovakia.

¹W. Braunish, N. Knauf, V. Kataev, S. Neuhausen, A. Grutz, A. Kock, B. Roden, D. Khomskii, and D. Wohlleben, *Phys. Rev. Lett.* **68**, 1908 (1992).

²Ch. Heinzl, Th. Theilig, and P. Ziemann, *Phys. Rev. B* **48**, 3445 (1993).

³F.V. Kusmartsev, *Phys. Rev. Lett.* **69**, 2268 (1992).

⁴M. Sigrist and T.M. Rice, *J. Phys. Soc. Jpn.* **61**, 4283 (1992).

⁵C. Tsuei and J.R. Kirtley, *Rev. Mod. Phys.* **72**, 969 (2000).

⁶D.J. Thompson, M.S.M. Minhaj, L.E. Wenger, and J.T. Chen, *Phys. Rev. Lett.* **75**, 529 (1995).

⁷A.K. Geim, S.V. Dubonos, J.G.S. Lok, M. Henini, and J.C. Maan, *Nature (London)* **396**, 144 (1998).

⁸T.M. Rice and M. Sigrist, *Phys. Rev. B* **55**, 14 647 (1997).

⁹J.R. Kirtley, A.C. Mota, M. Sigrist, and T.M. Rice, *J. Phys.: Condens. Matter* **10**, L97 (1998).

¹⁰E. Ilichev, V. Zakosarenko, L. Fritzsche, R. Stolz, H.E. Hoenig, H.-G. Meyer, M. Gotz, A.B. Zorin, V.V. Khanin, A.B. Pavlotsky, and J. Niemeyer, *Rev. Sci. Instrum.* **72**, 1882 (2001).

¹¹E. Il'ichev, M.V. Fistul, B.A. Malomed, H.E. Hoenig, and H.-G. Meyer, *Europhys. Lett.* **54**, 515 (2001).

¹²Q.D. Jiang, Z.J. Huang, A. Brazdeikis, M. Dezaneti, C.L. Chen, P. Jin, and C.W. Chu, *Appl. Phys. Lett.* **72**, 3365 (1998).

¹³H.J.H. Smilde, Ariando, D.H.A. Blank, G.J. Gerritsma, H. Hilgenkamp, and H. Rogalla, *Phys. Rev. Lett.* **88**, 057004 (2002).

¹⁴F. Tafuri, F. Miletto Granozio, F. Carillo, A. Di Chiara, K. Verbist, and G. Van Tendeloo, *Phys. Rev. B* **59**, 11 523 (1999).

¹⁵F. Tafuri, F. Carillo, F. Lombardi, F. Miletto Granozio, F. Ricci, U. Scotti di Uccio, A. Barone, G. Testa, E. Sarnelli, and J.R. Kirtley, *Phys. Rev. B* **62**, 14 431 (2000).

¹⁶F. Lombardi, F. Tafuri, F. Ricci, F. Miletto Granozio, A. Barone,

G. Testa, E. Sarnelli, J.R. Kirtley, and C.C. Tsuei, *Phys. Rev. Lett.* **89**, 207001 (2002).

¹⁷E. Il'ichev, V. Schultze, R.P.J. IJsselsteijn, R. Stolz, V. Zakosarenko, H.E. Hoenig, H.-G. Meyer, and M. Siegel, *Physica C* **330**, 155 (2000).

¹⁸J. Kurkijarvi, *Phys. Rev. B* **6**, 832 (1972).

¹⁹E. Il'ichev, V. Zakosarenko, V. Schultze, H.-G. Meyer, H.E. Hoenig, V.N. Glyantsev, and A. Golubov, *Appl. Phys. Lett.* **72**, 731 (1998).

²⁰R.G. Mints, *Phys. Rev. B* **57**, R3221 (1998).

²¹H. Hilgenkamp, J. Mannhart, and B. Mayer, *Phys. Rev. B* **53**, 14 586 (1996).

²²C.A. Copetti, F. Ruders, B. Oelze, Ch. Buchal, B. Kabius, and J.W. Seo, *Physica C* **253**, 63 (1995).

²³T. Löfwander, V.S. Shumeiko, and G. Wendin, *Phys. Rev. B* **62**, R14 653 (2000).

²⁴Y. Tanaka and S. Kashiwaya, *Phys. Rev. B* **56**, 892 (1997).

²⁵S. Higashitani, *J. Phys. Soc. Jpn.* **66**, 2556 (1997).

²⁶T. Löfwander, V.S. Shumeiko, and G. Wendin, *Semicond. Sci. Technol.* **14**, 53 (2001).

²⁷Chia-Ren Hu, *Phys. Rev. Lett.* **72**, 1526 (1994).

²⁸M. Sigrist, *Prog. Theor. Phys.* **99**, 899 (1998).

²⁹M.H.S. Amin, S.N. Rashkeev, M. Coury, A.N. Omelyanchouk, and A.M. Zagoskin, *Phys. Rev. B* **66**, 174515 (2002).

³⁰E. Il'ichev *et al.*, *Phys. Rev. Lett.* **86**, 5369 (2001).

³¹M. Covington, M. Aprili, E. Paraoanu, L.H. Greene, F. Xu, J. Zhu, and C.A. Mirkin, *Phys. Rev. Lett.* **79**, 277 (1997).

³²J. Mannhart, H. Hilgenkamp, B. Mayer, C. Gerber, J.R. Kirtley, K.A. Moler, and M. Sigrist, *Phys. Rev. Lett.* **77**, 2782 (1996).

³³J.R. Kirtley, P. Chaudhari, M.B. Ketchen, N. Khare, Shawn-Yu Lin, and T. Shaw, *Phys. Rev. B* **51**, R12 057 (1995).

³⁴F. Tafuri, J.R. Kirtley, F. Lombardi, and F. Miletto Granozio, *Phys. Rev. B* **67**, 174516 (2003).